

# Non-Fourier fractional thermoelastic two dimensional model of a hollow sphere

Vinayak Kulkarni<sup>1</sup> and Gaurav Mittal<sup>2</sup>

<sup>1</sup>University of Mumbai

<sup>2</sup>Thadomal Shahani Engineering College

April 28, 2020

## Abstract

Assuming non-Fourier thermal effects, Tzou's dual-phase-lag model has been applied to introduce the governing heat conduction equation in the presented mathematical model. Moreover, in order to design a well-posed stable dual-phase-lag model, the governing time fractional dual-phase-lag heat equation has been established by introducing conductive temperature and thermodynamical temperature, satisfying the two-temperature theory. Due to the application of phase-lags the heat conduction equation became hyperbolic. The corresponding governing equations of motion and stresses have been considered in two-dimensional bounded spherical domain. The spherical boundaries are assumed to be traction free. The Laplace and the Legendre integral transforms have been applied to obtain the analytical solutions of conductive and thermodynamical temperatures, displacement components and thermal stresses. The Gaver-Stehfest algorithm has been employed to achieve the time domain inversions of Laplace transforms numerically, satisfying the Kuznetsov convergence criteria. Classical, fractional and generalized thermoelasticity theories has been recovered theoretically and numerically as well for various fractional orders and phase-lags values.

## Hosted file

Manuscript.pdf available at <https://authorea.com/users/310858/articles/441601-non-fourier-fractional-thermoelastic-two-dimensional-model-of-a-hollow-sphere>

## 1. Introduction

According to the classical theory of thermoelasticity, it was presumed that the change in temperature of a solid due to external or internal thermal loading is independent of the mechanical forces applied to the solid body. Biot [1] has introduced coupled thermoelasticity theory, and claimed that thermal and mechanical forces applied to a solid are not independent rather these forces are dependent on each other. Assuming very small variations from the reference temperature, Chen and Gurtin [2] have designed two-temperature theory, using thermodynamical and conductive temperatures. Moreover, the coupled and two-temperature theories as well were not successfully able to achieve the finite speed of thermal wave propagation. Cattaneo [3] has introduced the relaxation time  $\tau$  and generalized the classical Fourier law of heat conduction. Following Cattaneo, Lord and Shulman [4] have derived the generalized coupled thermoelasticity by applying the relaxation time  $\tau$ , to the heat conduction equation and hence achieved the finite speed of thermal waves. To support the generalized theory of thermoelasticity Sherief et al. [5 – 6] have proved the uniqueness theorem and provided the corresponding fundamental solutions. Youssef [7] has generalized the two-temperature theory of thermoelasticity introduced by Chen and Gurtin [2], where due to the hyperbolic nature of the newly obtained heat conduction equation the finite speed of thermal wave propagation was achieved. Youssef has

also recovered the classical and coupled theories as a special case by using the generalized two-temperature theory. Tzou [8] has shown that Cattaneo-Vernotte constitutive relation has only taken account of the fast transient effects, but not the microstructural interactions. To investigate the lagging behaviour of the heat conduction, delay time translations  $\tau_\Omega$  and  $\tau_\Theta$ , to the heat flux vector  $\vec{Q}$  and temperature gradient  $\nabla T$  respectively and proposed the dual-phase-lag law of heat conduction. Quintanilla [9] has claimed that whenever a DPL is coupled with an energy equation, then the resulting heat conduction model could be unstable. Moreover, as per Quintanilla, under certain conditions, the dual-phase-lag heat conduction law could be made stable if coupled with the energy equation in the context of linearized two-temperature theory of thermoelasticity.

As per the various physical conditions, the upcoming states of every dynamical system does not depend on its present state; rather it is important to consider all of its previous states. Due to the non-local properties of fractional derivatives over classical integer order derivatives, scientists preferably uses arbitrary ordered derivatives to express various heat transfer problems, modelling of heat exchangers, categorization of various conducting materials to fabricate semiconductors, study the heating effects of thermoviscoelastic materials, magneto thermoelastic problems of heat conduction related problems from last so many years. This must be the reason why fractional calculus is becoming more popular in scientific research and modelling. Povstenko [10] has derived fractional heat conduction equation by replacement of ordinary derivative with respect to time variable by Caputo [11] time fractional derivative in classical Fourier law of heat conduction and initiated the fractional theory of thermoelasticity. Sherief et al. [12] have derived the fractional order theory of thermoelasticity in context with one relaxation time. Moreover, a brief discussion has been made for several limiting cases, followed by a uniqueness, reciprocity theorems and corresponding variational principle.

Sherief and Hamza [13] have formulated a two-dimensional thermoelastic problem under axisymmetric temperature distributions using generalized thermoelasticity with one relaxation time. The general solutions of temperature, thermal displacement components and thermal stresses were obtained in the Laplace domain by the direct method in the absence of the use of regular potential functions. The results were used to solve two problems of a stress-free solid sphere and a spherical cavity of infinite space subjected to axisymmetric thermal distribution. Recently, Mittal and Kulkarni [14] have derived a fractionally ordered dual-phase-lag heat conduction equation in the context of the two-temperature theory of thermoelasticity. The formulation has been implemented to a one dimensional hollow sphere whose boundary surfaces were free of mechanical loading and subjected to external heat flux. The analytical results were obtained in the Laplace domain, where corresponding inversions were computed for various phase-lags, fractional orders. The classical, generalized cases were recaptured.

Following Mittal and Kulkarni [14] the piece of work presented has been reconstructed as a two dimensional model in the bounded spherical domain. The boundary surfaces of the hollow sphere are traction free and subjected to sinusoidal heat flux. The governing heat conduction equation has been derived using Tzou dual-phase-lag intuitive law of heat conduction where two different translations  $\tau_\Omega, \tau_\Theta$  are called phase-lags, that has been applied to heat flux vector and temperature gradient respectively. The governing equations of motion, thermal stresses have been given in the two-dimensional bounded spherical domain. The analytical solutions of non-dimensional governing equations subject to boundary conditions have been obtained using the Laplace and the Legendre integral transforms. The numerical inversion of the Laplace transform has been obtained using the Gaver-Stehfest algorithm [15, 16]. The Legendre inversions involved in results has been computed in terms of the Legendre polynomials for a specified Legendre parameter. The numerical solutions have been plotted in radial direction considering the various phase-lags case and different fractional orders. The results obtained have been compared with classical and generalized thermoelasticity theories.

The materials like glass, ceramics, polymers, steel become brittle due to application of stress occurring either due to thermal loading or pressure etc. applied to the surface. Galanov et al. [17] have presented a model describing the elastic deformations of spherical cavity developed in the brittle materials using the concept of mechanics of compressive porous and powder materials. Marin et al. [18] have investigated the theory of micropolar thermoelastic bodies whose micro-particles possess microtemperature. The mixed initial boundary value problem has been converted into a temporally evolutionary equation on a Hilbert space. The solution

obtained has been examined for its existence and uniqueness.

The presented dual-phase-lag heat conduction model has been constructed using the two-temperature theory to investigate the thermal effects of microstructural interactions occurring inside the hollow sphere whose boundaries are subjected to sinusoidal heat flux. This model could be employed to classify the various conducting materials as per their conductive capacity by using either phase-lags or fractional order variations. To the best of authors knowledge so far no one has designed a two dimensional fractional dual-phase-lag heat conduction model in the context of two-temperature theory within the bounded spherical domain. This is the newest and novel contribution to the field of material science.

2

## Nomenclature

$\beta$	: Fractional order;
$\alpha_t$	: Coefficient of linear thermal expansion;
$\xi$	: Temperature discrepancy;
$\eta$	: Reciprocal of thermal diffusivity;
$\epsilon$	: Dimensionless coupling constant;
$\mathbb{k}$	: Thermal conductivity;
$\lambda, \mu$	: Lamé constants ;
$\gamma = \alpha_t(3\lambda + 2\mu)$	: Material constant;
$\varphi$	: Thermodynamical temperature;
$\vartheta$	: Non-dimensional thermodynamical temperature;
$\rho_d$	: Material density;
$\sigma_{ij}$	: Thermal stresses;
$\Theta$	: Non-dimensional conductive temperature;
$P$	: The position vector;
$H$	: Internal heat generation;
$T$	: Conductive temperature;
$T_0$	: Reference temperature;
$c$	: Constant of two temperature theory;
$\tau$	: Relaxation time;
$\tau_\Theta, \tau_\Omega$	: Phase-Lags;
$c_e$	: Speed of iso-thermal elastic wave;
$c_s$	: Specific heat capacity;
$e$	: Cubical dilatation;
$\vec{\Omega}$	: Heat flux vector;
$u_r, u_\theta$	: Displacement Components;
$t$	: Time;
$(r, \theta, \phi)$	: Spherical coordinate system;
$\nabla$	: Gradient operator;
$\nabla^2$	: Laplacian operator.

## 2. The heat conduction equation

Since the governing heat equation of classical thermoelasticity, results an infinite speed of thermal wave propagation, this must be the reason why, Lord and Shulman [4] has applied Maxwell-Cattaneo law with one relaxation time and derived the generalized coupled heat conduction equation given by

$$\left(1 + \tau \frac{\partial}{\partial t}\right) \left\{ \frac{\partial}{\partial t} (\rho_d c_s T + \gamma T_0 e) - H \right\} = \mathbb{k} \nabla^2 T, \quad (1)$$

Following Caputo time fractional derivative [11] of order  $\beta \in (0, 1]$ , Sherief et al. [12] have updated the generalized theory of thermoelasticity as

$$\left(1 + \tau \frac{\partial^\beta}{\partial t^\beta}\right) \left\{ \frac{\partial}{\partial t} (\rho_d c_s T + \gamma T_0 e) - H \right\} = \mathbb{k} \nabla^2 T, \quad (2)$$

To investigate the consequences of small scale inner particle communications aroused within the solid heat conductor at a microscopic level, Tzou [8] has considered the non-Fourier effects of heating and proposed the dual-phase-lag law given below

$$\vec{\Omega}(P, t + \tau_\Omega) = -\mathbb{k} \nabla T(P, t + \tau_\Theta), \quad (3)$$

where,  $\tau_\Omega$  and  $\tau_\Theta$  are the intrinsic properties of the medium. Expanding both sides of equation (3) using Taylor's series with respect to the time fractional derivatives till  $2\beta$  and taking divergence, one obtains

Moreover, Quintanilla [9] has claimed that, if equation (4) couples with the energy equation given by

$$-\nabla \vec{\Omega}(P, t) = d\dot{T}(P, t), \quad (4)$$

then consequently, Tzou's [8] DPL model would be ill-posed and not stable. Moreover, under certain physical restrictions, a DPL could also be made stable and well-posed if derived in the context of two-temperature theory where two different temperatures are known as thermodynamical temperature  $\varphi$  and conductive temperature  $T$ , satisfies

Coupling the equation (4) and (6) and neglecting the differential operators of order more than  $\nabla^2$ , one will have the following time fractional dual-phase-lag heat conduction equation in the context of two-temperature theory given by

## 2.1 Specific cases

**a.** For  $[\tau_{\Theta} = \tau_{\Omega} = 0, T = \varphi, H = 0]$ , equation (7) represents the heat conduction equation of Biot's theory shown below

**b.** For  $[\beta \rightarrow 1.0, \tau_{\Theta} = 0, \tau_{\Omega} = \tau > 0, \tau_{\Omega}^2 \rightarrow 0, T = \varphi, H = 0]$ , equation (7) expresses the heat conduction equation of Lord-Shulman thermoelasticity as follows

**c.** For  $[\beta \in (0, 1), T = \varphi, H = 0]$ , equation (7) is identified as the fractional generalization of Cattaneo approach.

**d.** For  $[\beta \rightarrow 0.0, \tau_{\Theta}, \tau_{\Omega} \in, T \neq \varphi]$ , equation (7) stands for governing equation of the generalized two-temperature theory of thermoelasticity derived by Youssef [7] as

**e.** For  $[\beta \in (0, 1), \tau_{\Theta} = 0, \tau_{\Omega} \equiv \tau, \tau_{\Omega}^2 \rightarrow 0, T \neq \varphi]$ , equation (7) converts as

equation (11) represents two-temperature thermoelastic models proposed by Ezzat and Karamany [19, 20].

## 2.2 Mathematical model

Assume a spherically symmetrical, isotropic, homogeneous and ideally thermoelastic medium, where a hollow sphere has been placed with traction free boundary surfaces. The object under study is supposed to occupy the space  $S \subset^3$  in the bounded spherical domain as shown below

where  $a$  and  $b$  are the positive real number represents the radius of inner and outer spherical boundaries. For the sake of mathematical simplicity it has been assumed that, there is neither external body force has

been applied to the solid nor the per unit volume heat has been generated inside the solid. For ( $H = 0$ ), the heat conduction equation (7) reduces to

where  $\nabla^2$  is two dimensional Laplacian operator in spherical domain has the form

Following Eslami et al. [21], for the displacement  $\vec{U} = (u_r, u_\theta, 0)$ , the strain components are given as

$$e_{rr} = \frac{\partial u_r}{\partial r}, \quad (5)$$

$$e_{\theta\theta} = \frac{1}{r} \frac{\partial u_\theta}{\partial \theta} + \frac{u_r}{r}, \quad (6)$$

$$e_{\phi\phi} = \frac{\cot \theta}{r} u_\theta + \frac{u_r}{r}, \quad (7)$$

$$e_{r\theta} = \frac{1}{2} \left[ \frac{u_\theta}{r} + \frac{1}{r} \left( \frac{\partial u_r}{\partial \theta} - u_\theta \right) \right], \quad (8)$$

Thus the cubical dilatation  $e$  takes the form

$$e = e_{rr} + e_{\phi\phi} + e_{\theta\theta}, \quad (9)$$

Considering no external forces applied to the body then the equation of motion are reduces to

$$(\lambda + 2\mu)\frac{\partial e}{\partial r} - \frac{2\mu}{r \sin \theta} \frac{\partial}{\partial \theta} \left[ \frac{1}{2r} \left( r \frac{\partial u_\theta}{\partial r} + u_\theta - \frac{\partial u_r}{\partial \theta} \right) \sin \theta \right] - \gamma \frac{\partial}{\partial r} (T - T_0) = \rho_d \frac{\partial^2 u_r}{\partial t^2}, \quad (10)$$

The normal and shear stress functions are expressed by following equations

$$\sigma_{rr} = 2\mu \frac{\partial u_r}{\partial r} + \lambda e - \gamma(T - T_0), \quad (11)$$

$$\sigma_{\theta\theta} = 2\mu \left( \frac{u_r}{r} + \frac{1}{r} \frac{\partial u_\theta}{\partial \theta} \right) + \lambda e - \gamma(T - T_0), \quad (12)$$

$$\sigma_{\phi\phi} = 2\mu \left( \frac{u_r}{r} + \cot \theta \frac{u_\theta}{r} \right) + \lambda e - \gamma(T - T_0), \quad (13)$$

$$\sigma_{r\theta} = \mu \left[ \frac{u_\theta}{r} + \frac{1}{r} \left( \frac{\partial u_r}{\partial \theta} - u_\theta \right) \right], \quad (14)$$

$$\sigma_{r\phi} = \sigma_{\theta\phi} = 0. \quad (15)$$

Equations (12) – (28) describes the governing equations of heat conduction model for hollow spherical region.

## 2.3 Non-dimensional governing equations

To convert the dimensionless system of governing equations the following non-dimensional quantities are introduced as

The dimensionless form of the governing equations of the model are given below (dropping asterisk sign for simplicity)

$$\Theta - \vartheta = \xi \nabla^2 \Theta, \quad (16)$$

$$e = \frac{\partial u_r}{\partial r} + 2 \frac{u_r}{r} + \cot \theta \frac{u_\theta}{r} + \frac{1}{r} \frac{\partial u_\theta}{\partial \theta}, \quad (17)$$

$$\frac{\partial}{\partial r} [\alpha^2 e - \wp \Theta] + \nabla^2 u_r - \frac{1}{r^2} \frac{\partial}{\partial r} \left[ r^2 \frac{\partial u_r}{\partial r} \right] - \frac{1}{r^2 \sin \theta} \frac{\partial^2}{\partial r \partial \theta} [r \sin \theta u_\theta] = \alpha^2 \frac{\partial^2 u_r}{\partial t^2}, \quad (18)$$

$$\frac{1}{r} \frac{\partial}{\partial \theta} \left[ \alpha^2 e - \wp \Theta - \frac{\partial u_r}{\partial r} \right] + \frac{1}{r^2} \frac{\partial}{\partial r} \left[ r^2 \frac{\partial u_\theta}{\partial r} \right] = \alpha^2 \frac{\partial^2 u_\theta}{\partial t^2}, \quad (19)$$

$$\sigma_{rr} = 2 \frac{\partial u_r}{\partial r} + (\alpha^2 - 2) e - \alpha^2 \Theta, \quad (20)$$

$$\sigma_{\theta\theta} = 2 \left( \frac{\partial u_r}{\partial r} + \frac{1}{r} \frac{\partial u_\theta}{\partial \theta} \right) + (\alpha^2 - 2) e - \alpha^2 \Theta, \quad (21)$$

$$\sigma_{\phi\phi} = 2 \left( \frac{u_r}{r} + \cot \theta \frac{u_\theta}{r} \right) + (\alpha^2 - 2) e - \alpha^2 \Theta, \quad (22)$$

$$\sigma_{r\theta} = \frac{1}{r} \frac{\partial u_r}{\partial \theta} - \frac{u_\theta}{r} + \frac{\partial u_\theta}{\partial r}. \quad (23)$$

Equations (29) – (38) represents the dimensionless form of the governing equations.

## 2.4 Physical restrictions

The spherical boundary surfaces of hollow sphere are subjected to sinusoidal heat flux  $\Theta(r, \theta, t)$  given below:

$$\begin{cases} 0, & r = a, \\ \Theta_0 \sin \theta H(t) & r = b, \end{cases}$$

where  $-\pi \leq \theta \leq \pi$ , and constant  $\Theta_0$  stands for the strength of the heat flux applied.

Mathematically, the stress free boundary conditions are defined as follows

$$\sigma_{rr} = \sigma_{\theta\theta} = \sigma_{r\theta} = 0|_{r=a}, \quad (24)$$

Assuming quiescent state, the initial conditions are given as

$$\Theta(r, \theta, 0) = \dot{\Theta}(r, \theta, 0) = 0, \quad (25)$$

$$\sigma_{rr}(r, 0) = \dot{\sigma}_{rr}(r, 0) = 0, \quad (26)$$

Equations (39) – (44) describe the physical restrictions imposed on the mathematical model of the hollow sphere in the bounded spherical domain.

### 3. Mathematical treatment

#### 3.1 Transformation in the Laplace domain

**Theorem :** Following Liang et al. [22], if  $\beta > 0$ ,  $m = [\beta] + 1$ , and functions  $\omega(P, t)$  and its partial derivatives up to the order  $(m - 1)$  with respect to the variable  $t$  exists and continuous in  $+$  are of exponential order, where  ${}^C D_0^\beta \omega(t)$  of fractional order  $\beta$  is piecewise continuous in  $+$ , then the Laplace transform of  ${}^C D_0^\beta \omega(t)$  is given by

For the Liang theorem described above, considering zero initial conditions one must have the following equation

Using equations (45) – (46), applying the Laplace transforms to the dimensionless governing equations (30) – (38) the transformed equations are given as

$$\bar{\Theta} - \bar{\vartheta} = \xi \nabla^2 \bar{\Theta}, \quad (27)$$

$$\bar{e} = \frac{du_r}{dr} + 2\frac{\bar{u}_r}{r} + \cot \theta \frac{\bar{u}_\theta}{r} + \frac{1}{r} \frac{d\bar{u}_\theta}{d\theta}, \quad (28)$$

$$\frac{d}{dr} [\alpha^2 \bar{e} - \wp \bar{\Theta}] + \nabla^2 \bar{u}_r - \frac{1}{r^2} \frac{d}{dr} \left[ r^2 \frac{d\bar{u}_r}{dr} \right] - \frac{1}{r^2 \sin \theta} \frac{d^2}{dr d\theta} [r \sin \theta \bar{u}_\theta] = \alpha^2 p^2 \bar{u}_r, \quad (29)$$

$$\frac{1}{r} \frac{d}{d\theta} \left[ \alpha^2 \bar{e} - \wp \bar{\Theta} - \frac{d\bar{u}_r}{dr} \right] + \frac{1}{r^2} \frac{d}{dr} \left[ r^2 \frac{d\bar{u}_\theta}{dr} \right] = \alpha^2 p^2 \bar{u}_\theta, \quad (30)$$

$$\bar{\sigma}_{rr} = 2 \frac{d\bar{u}_r}{dr} + (\alpha^2 - 2) \bar{e} - \alpha^2 \bar{\Theta}, \quad (31)$$

$$\bar{\sigma}_{\theta\theta} = 2 \left( \frac{d\bar{u}_r}{dr} + \frac{1}{r} \frac{d\bar{u}_\theta}{d\theta} \right) + (\alpha^2 - 2) \bar{e} - \alpha^2 \bar{\Theta}, \quad (32)$$

$$\bar{\sigma}_{\phi\phi} = 2 \left( \frac{\bar{u}_r}{r} + \cot \theta \frac{\bar{u}_\theta}{r} \right) + (\alpha^2 - 2) \bar{e} - \alpha^2 \bar{\Theta}, \quad (33)$$

$$\bar{\sigma}_{r\theta} = \frac{1}{r} \frac{d\bar{u}_r}{d\theta} - \frac{\bar{u}_\theta}{r} + \frac{d\bar{u}_\theta}{dr}, \quad (34)$$

Combining the equations (50) and (51) one will have

where  $\varsigma = \frac{\wp}{\alpha^2}$ .

Consider the following term replacements

$$\Omega_1 = \left[ p + p^{\beta+1} \frac{\tau_{\Omega}^{\beta}}{\Gamma(\beta+1)} + p^{2\beta+1} \frac{\tau_{\Omega}^{2\beta}}{\Gamma(2\beta+1)} \right], \quad (35)$$

$$\Omega_2 = \left[ 1 + p^{\beta} \frac{\tau_{\Theta}^{\beta}}{\Gamma(\beta+1)} + p^{2\beta} \frac{\tau_{\Theta}^{2\beta}}{\Gamma(2\beta+1)} \right]. \quad (36)$$

Using the above replacements equation (47) reduces to

$$\Omega_2 \nabla^2 \bar{\Theta} = \Omega_1 (\bar{\vartheta} + \epsilon \bar{e}), \quad (37)$$

Eliminating  $\vartheta$  and  $\Theta$  between the equations (59) – (60) in context of equation (48), one obtains the following differential equation for  $\bar{e}$  given below:

Equation (60) can be factored as

where  $q_1^2, q_2^2$  are the positive real roots of the following characteristic equation

where

$$L = \frac{p^2 \Omega_1 \xi + \Omega_2 p^2 + \varsigma \Omega_1 \epsilon + \Omega_1}{\Omega_1 \xi + \Omega_2}, \quad (38)$$

Equations (47) – (64) represents the dimensionless governing equations in the Laplace domain.

### 3.2 Analytical results in the Laplace domain

The analytical solutions of conductive temperature, thermodynamical temperature, displacement components and thermal stresses has been achieved through the application of Legnedre transform to the equations (47)-(64) in the variables  $p$ ,  $r$  and  $\zeta = \cos \theta$ .

Solving equation (61), the dilatation function  $\bar{e}(r, p, \zeta)$  is given as

$$\bar{e}(r, p, \zeta) = \bar{e}_1(r, p, \zeta) + \bar{e}_2(r, p, \zeta), \quad (39)$$

The functions  $\bar{e}_1(r, p, \zeta)$ ,  $\bar{e}_2(r, p, \zeta)$  are components of dilatation function bounded at origin and infinity respectively.

Substituting results from equations (66)–(67) to equation (56) the conductive temperature function  $\bar{\Theta}(r, p, \zeta)$  in the Laplace domain is given as

where

The functions  $\bar{\Theta}_1(r, p, \zeta)$ ,  $\bar{\Theta}_2(r, p, \zeta)$  are components of conductive temperature function  $\bar{\Theta}$  bounded at origin and infinity respectively.

Substituting components of conductive temperature  $\bar{\Theta}_1(r, p, \zeta)$ ,  $\bar{\Theta}_2(r, p, \zeta)$  from equations (69)–(70) in two-temperature theory relation given by equation (48), one gets the thermodynamical temperature  $\bar{\vartheta}(r, p, \zeta)$  as given below:

where

The functions  $\bar{\vartheta}_1(r, p, \zeta), \bar{\vartheta}_2(r, p, \zeta)$  are components of conductive temperature function  $\bar{\vartheta}(r, p, \zeta)$  bounded at origin and infinity respectively.

The radial displacement  $\bar{u}_r(r, p, \zeta)$  is given by

where

$$\bar{u}_{r1}(r, p, \zeta) = \frac{S}{r^{3/2}} \sum_{m=0}^{\infty} \left\{ \sum_{i=1}^2 P_m(\zeta) A_{mi} [q_i r I_{m+3/2}(q_i r) + m I_{m+1/2}(q_i r)] + I_{m+1/2}(\alpha p r) \right\}, \quad (40)$$

Similarly following mathematical equation (32), displacement component  $u_\theta(r, p, \zeta)$  has been obtained

where

$$\bar{\psi}_1(r) = A_{mi} m(m+1) I_{m+1/2}(q_i r) + C_m [(m+1) I_{m+1/2}(\alpha p r) + \alpha p r I_{m+3/2}(\alpha p r)], \quad (41)$$

On integrating equation (77), using  $\int P_m(\zeta)d\zeta = \frac{\zeta P_m(\zeta) - P_{m-1}(\zeta)}{(m+1)}$ , one gets

where the displacement component  $u_\theta$  is given as

The stress functions are obtained by substituting the above results of dilatation, temperature and displacement functions to the equations (35) – (38), one will have the following results for radial stresses given below:

where

Similarly the shear stress  $\bar{\sigma}_{r\theta}(r, p, \zeta)$  is given by

where

Likewise, one gets  $\bar{\sigma}_{\theta\theta}(r, p, \zeta)$  as given below:

where

Finally the hoop stress  $\bar{\sigma}_{\phi\phi}(r, p, \zeta)$  is obtained as under,

where,

To fix the constants  $A_{mi}(p), B_{mi}(p), C_m(p), D_m(p)$  depending upon the Laplace parameter  $p$ , one will make use of boundary conditions to obtain the simultaneous equations given below:

Equations (65) – (98) represents analytical solutions obtained for conductive temperature  $\Theta(r, p, \zeta)$ , thermodynamical temperature  $\vartheta(r, p, \zeta)$ , displacement components  $u_r(r, p, \zeta)$ ,  $u_\theta(r, p, \zeta)$  and stresses  $\bar{\sigma}_{rr}(r, p, \zeta)$ ,  $\bar{\sigma}_{\theta\theta}(r, p, \zeta)$ ,  $\bar{\sigma}_{\phi\phi}(r, p, \zeta)$  in the Laplace domain. Here  $I_m(\cdot), K_m(\cdot)$  denotes modified Bessel functions of first and second kind respectively and  $P_m(\zeta)$  denotes the Legendre polynomial of order  $m$  of argument  $\zeta = \cos \theta$  lying between  $[-1, 1]$  and  $p$  is the Laplace domain parameter.

### 3.3 The Gaver-Stehfest algorithm

Finally in order to find the results for conductive temperature, thermodynamical temperature, radial and angular displacement components of thermal stresses in the time domain, the inversion of the Laplace transform of analytical results obtained in the equations (65) – (98) has been carried out numerically by the Gaver-Stehfest algorithm.

Following the Gaver Stehfest [15, 16], the numerical inversion of the analytical results in the Laplace domain has been approximated to the time domain solutions as

$$f(t) \approx f_K(t) = \frac{\log_e(2)}{t} \sum_{k=1}^{2K} \left[ (-1)^{K+k} \left\{ \sum_{l=\left\lfloor \frac{k+1}{2} \right\rfloor}^{l=\min(k,K)} \frac{l^{K+1} \cdot {}^K C_l \cdot 2^l C_l \cdot {}^l C_{k-l}}{K!} \right\} \cdot F\left(\frac{k \log_e(2)}{t}\right) \right], \quad (42)$$

and  $\lfloor y \rfloor$  is the flooring function and  $2K$  is an even integer whose value depends on the word length of the computer used.

The Gaver-Stehfest algorithm discussed above has been implemented using Matlab 6.1. The trial value of  $K$  depending upon the word length of the computer system has been fixed as  $K = 12$ . Assuming the constant physical properties of the medium described in section 4.2, the starting iteration value for the Laplace parameter  $p$  has been obtained for  $K = 0$ , for the small input of fixed time value  $t = 0.2s$ . An initial solution of resulting thermal parameters of the Laplace domain shown by the equations (65) – (98) have been computed for starting numerical value of the Laplace parameter  $p$  for  $K = 0$ . This iteration process has been repeated to cumulate the values of the required Laplace inversions given in terms of the infinite series of modified Bessel functions for all values of  $K$  ranging from 0 to 12. Finally the infinite series representing the thermal results have been approximated to achieve the finite numerical values of the inverse Laplace transform, where only the real values of the Laplace inversions have been considered for concerned thermal parameters.

The convergence of the numerical inversion described by the Gaver-Stehfest algorithm has been discussed by Kuznetsov [23].

**The Kuznetsov convergence criterion :** If  $f : (0, \infty) \rightarrow \mathbb{R}$  is a locally integrable function such that its Laplace transform  $F(p)$  exists for all  $p > 0$  and the sequence  $f_K(t)$  is defined by equation (99), then the convergence of sequence  $f_K(t)$  depends on the values of the function  $f(t)$  in the neighbourhood of  $t$ . If the function  $f(t)$  is of bounded variation in the neighbourhood of  $t$  then the sequence  $f_K(t) \rightarrow \frac{f(t+0) + f(t-0)}{2}$  as  $K \rightarrow \infty$ .

Referring above Kuznetsov convergence criterion, it has been observed that as  $K$  increases, the resulting numerical values of the Laplace inversions are found to be stable and convergent to the finite real number. Accordingly  $K = 12$  has been chosen in the Matlab programming.

## 4. Numerical scheme

Mathematically, one can say that the distribution of temperature and thermal stresses inside the hollow spherical region subjected to fixed external heat flux is always influenced by variations of phase-lags. Additionally, as per fractional order theory proposed by Sherief et al. [12], the importance of fractional order applied to time variable to the governing dual-phase-lag heat conduction equation could not be ignored.

Therefore the numerical calculations have been carried out for conductive temperature  $\Theta$ , thermodynamical temperature  $\vartheta$ , displacement components  $u_r, u_\theta$  and stresses  $\sigma_{rr}, \sigma_{\theta\theta}, \sigma_{\phi\phi}, \sigma_{r\theta}$  by considering classical, fractional and generalized theory of thermoelasticity. Following Ignaczak and Ostoja-Starzewski [24], the results have been computed for various phase-lags by fixing ( $\beta = 0.45, 0.90$ ) and referring fractional theory of thermoelasticity by Povstenko [25] for different fractional orders ( $\tau_\Omega = 0.4ps, \tau_\Theta = 0.2ps$ ) and shown pairwise respectively by figures 1 – 8, for each thermal parameter under consideration at time  $t = 0.2s$ .

### 4.1 The dimensions

The inner radius of hollow sphere  $a = 0.02 m$ .  
The outer radius of hollow sphere  $b = 0.07 m$ .

### 4.2 Material characteristics

Following Luecke et al. [26] and Childs et al. [27], the numerical scheme has been applied to find the non-dimensional thermal variations for pure steel material with physical characteristics in (**SI-units**) given as

### 4.3 Results and discussion

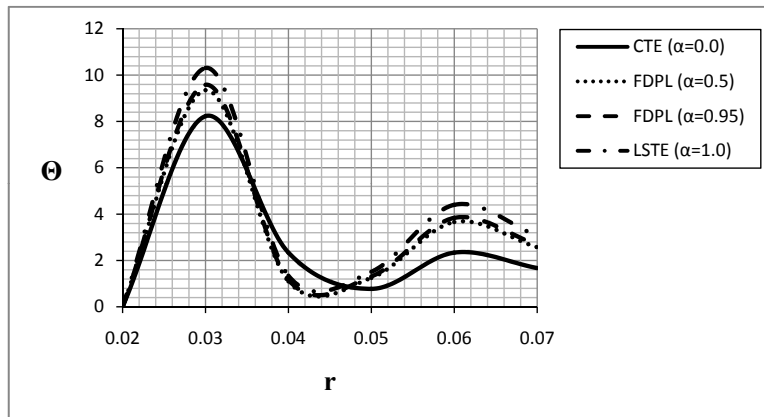
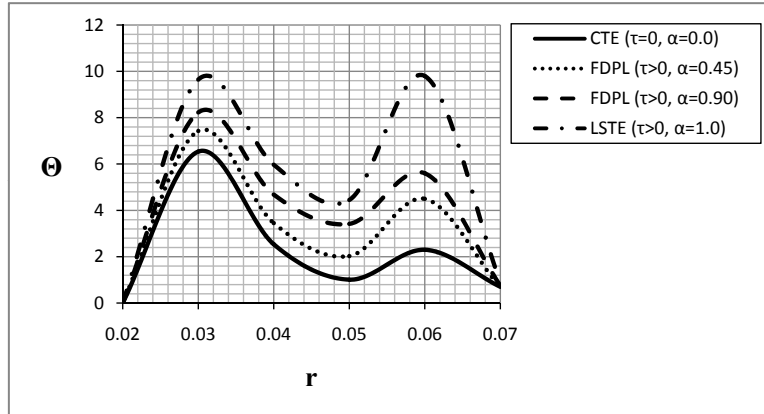


**Fig: 1(a).** Distribution of conductive temperature  $\Theta(r, \theta, t)$  inside the hollow sphere for phase-lag variations

**CTE theory**  $\tau = 0, \tau_{\Omega} = \tau_{\Theta} = 0,$

**FDPL theory**  $\tau > 0, \tau_{\Omega} = 0.4ps, \tau_{\Theta} = 0.2ps, \beta = 0.45,$

**FDPL theory**  $\tau > 0, \tau_{\Omega} = 0.4ps, \tau_{\Theta} = 0.2ps, \beta = 0.90,$

**LS theory**  $\tau > 0, \tau_{\Omega} = 0.4ps, \tau_{\Theta} = 0.$

**Fig: 1(b).** Distribution of conductive temperature  $\Theta(r, \theta, t)$  inside the hollow sphere for time-fractional derivative order  $\beta$

for  $\tau = \tau_{\Omega} - \tau_{\Theta} > 0, \tau_{\Theta} = 0.2ps, \tau_{\Omega} = 0.4ps.$

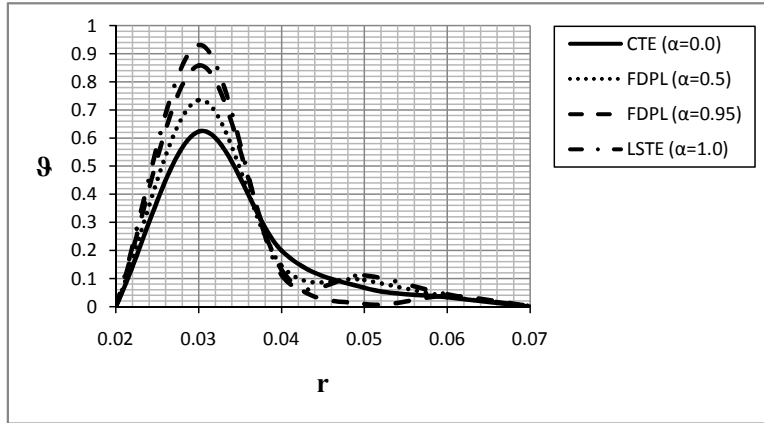
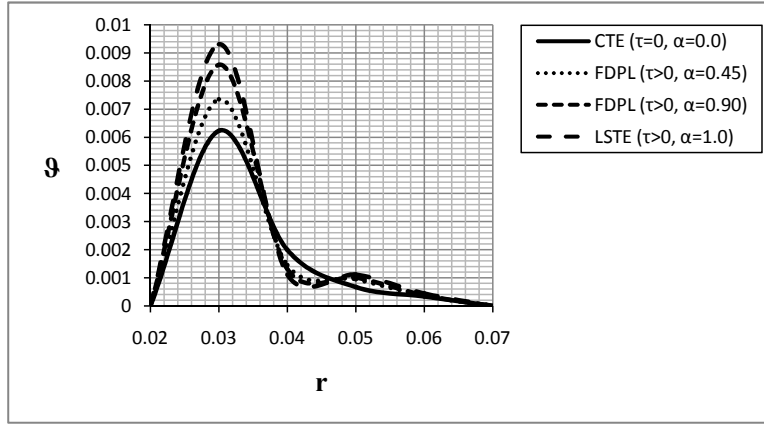


**Fig: 2(a).** Distribution of thermodynamical temperature  $\vartheta(r, \theta, t)$  inside the hollow sphere for phase-lag variations

**CTE theory**  $\tau = 0, \tau_{\Omega} = \tau_{\Theta} = 0,$

**FDPL theory**  $\tau > 0, \tau_{\Omega} = 0.4ps, \tau_{\Theta} = 0.2ps, \beta = 0.45,$

**FDPL theory**  $\tau > 0, \tau_{\Omega} = 0.4ps, \tau_{\Theta} = 0.2ps, \beta = 0.90,$

**LS theory**  $\tau > 0, \tau_{\Omega} = 0.4ps, \tau_{\Theta} = 0.$

**Fig: 2(b).** Distribution of thermodynamical temperature  $\vartheta(r, \theta, t)$  inside the hollow sphere for time-fractional derivative order  $\beta$  for  $\tau = \tau_{\Omega} - \tau_{\Theta} > 0, \tau_{\Theta} = 0.2ps, \tau_{\Omega} = 0.4ps.$

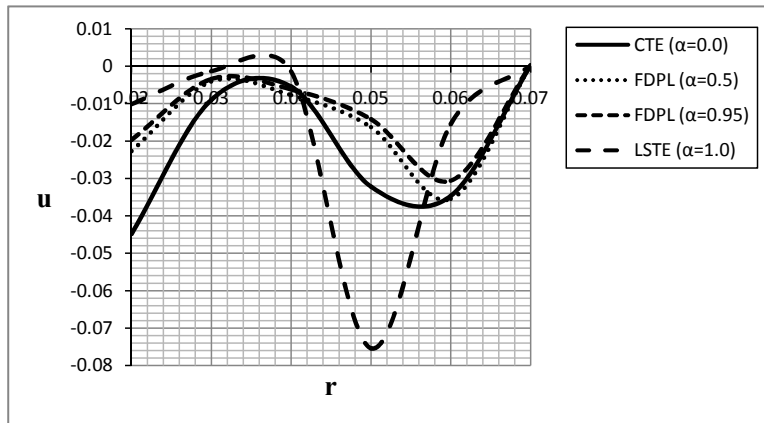
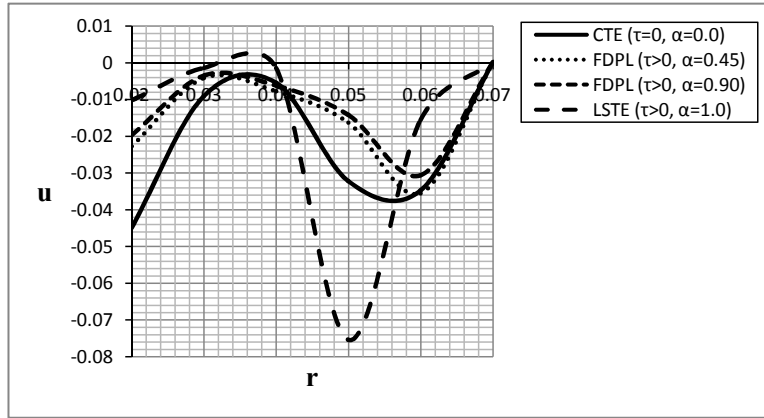


**Fig: 3(a).** Distribution of radial displacement component  $u_r(r, \theta, t)$  inside the hollow sphere for phase-lag variations

**CTE theory**  $\tau = 0, \tau_\Omega = \tau_\Theta = 0,$

**FDPL theory**  $\tau > 0, \tau_\Omega = 0.4ps, \tau_\Theta = 0.2ps, \beta = 0.45$

**FDPL theory**  $\tau > 0, \tau_\Omega = 0.4ps, \tau_\Theta = 0.2ps, \beta = 0.90$

**LS theory**  $\tau > 0, \tau_\Omega = 0.4ps, \tau_\Theta = 0.$

**Fig: 3(b).** Distribution of radial displacement component  $u_r(r, \theta, t)$  inside the hollow sphere for time-fractional derivative order  $\beta$

for  $\tau = \tau_\Omega - \tau_\Theta > 0, \tau_\Theta = 0.2ps, \tau_\Omega = 0.4ps.$

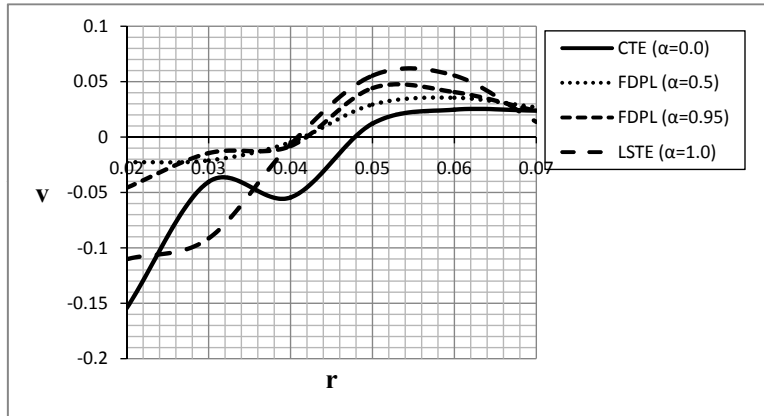
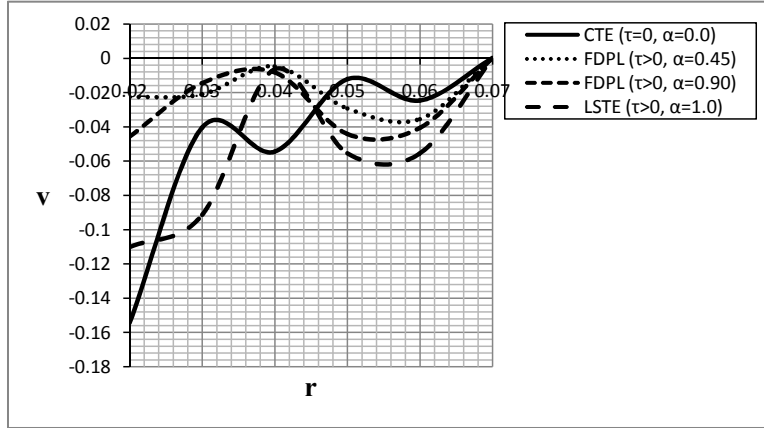


**Fig: 4(a).** Distribution of angular displacement component  $v_{\theta}(r, \theta, t)$  inside the hollow sphere for phase-lag variations

**CTE theory**  $\tau = 0, \tau_{\Omega} = \tau_{\Theta} = 0,$

**FDPL theory**  $\tau > 0, \tau_{\Omega} = 0.4ps, \tau_{\Theta} = 0.2ps, \beta = 0.45,$

**FDPL theory**  $\tau > 0, \tau_{\Omega} = 0.4ps, \tau_{\Theta} = 0.2ps, \beta = 0.90,$

**LS theory**  $\tau > 0, \tau_{\Omega} = 0.4ps, \tau_{\Theta} = 0.$

**Fig: 4(b).** Distribution of angular displacement component  $v_{\theta}(r, \theta, t)$  inside the hollow sphere for time-fractional derivative order  $\beta$

for  $\tau = \tau_{\Omega} - \tau_{\Theta} > 0, \tau_{\Theta} = 0.2ps, \tau_{\Omega} = 0.4ps.$

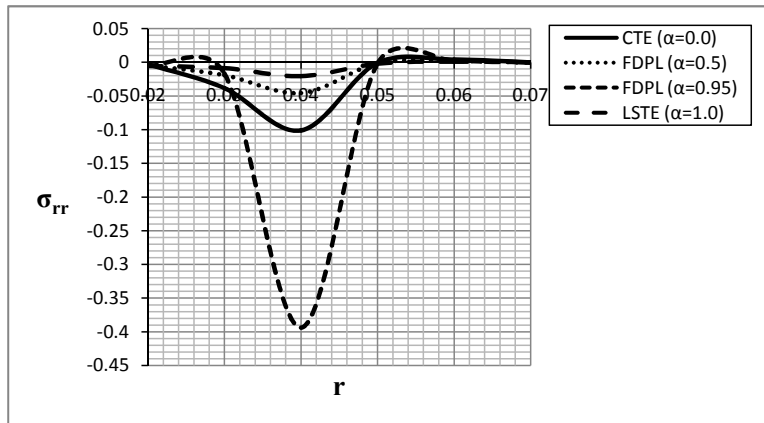
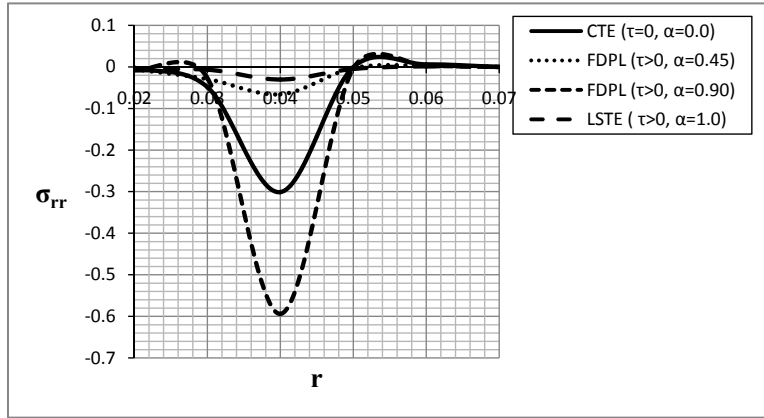


**Fig: 5(a).** Distribution of radial stress component  $\sigma_{rr}(r, \theta, t)$  inside the hollow sphere for phase-lag variations

**CTE theory**  $\tau = 0, \tau_{\Omega} = \tau_{\Theta} = 0,$

**FDPL theory**  $\tau > 0, \tau_{\Omega} = 0.4ps, \tau_{\Theta} = 0.2ps, \beta = 0.45,$

**FDPL theory**  $\tau > 0, \tau_{\Omega} = 0.4ps, \tau_{\Theta} = 0.2ps, \beta = 0.90,$

**LS theory**  $\tau > 0, \tau_{\Omega} = 0.4ps, \tau_{\Theta} = 0.$

**Fig: 5(b).** Distribution of radial stress component  $\sigma_{rr}(r, \theta, t)$  inside the hollow sphere for time-fractional derivative order  $\beta$

for  $\tau = \tau_{\Omega} - \tau_{\Theta} > 0, \tau_{\Theta} = 0.2ps, \tau_{\Omega} = 0.4ps.$

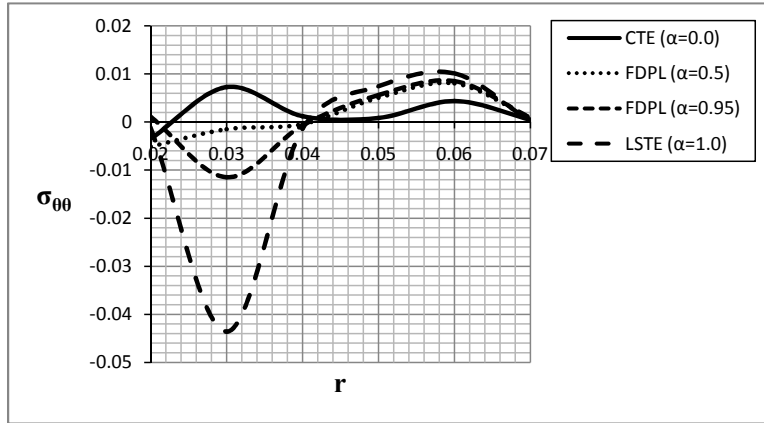
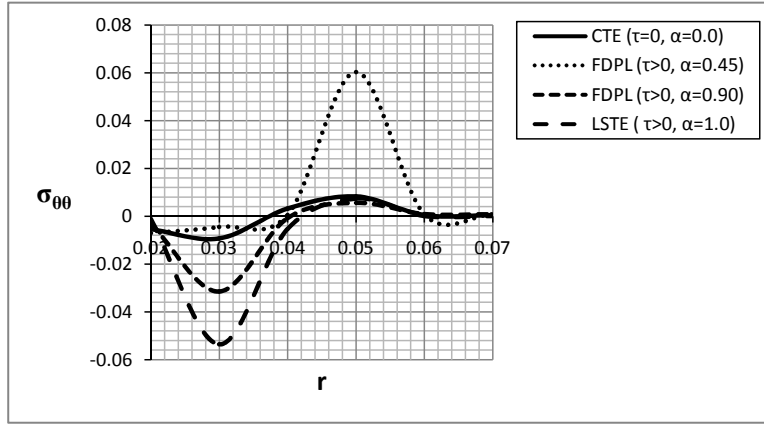


**Fig: 6(a).** Distribution of hoop stress component  $\sigma_{\theta\theta}(r, \theta, t)$  inside the hollow sphere for phase-lag variations

**CTE theory**  $\tau = 0, \tau_{\Omega} = \tau_{\Theta} = 0,$

**FDPL theory**  $\tau > 0, \tau_{\Omega} = 0.4ps, \tau_{\Theta} = 0.2ps, \beta = 0.45,$

**FDPL theory**  $\tau > 0, \tau_{\Omega} = 0.4ps, \tau_{\Theta} = 0.2ps, \beta = 0.90,$

**LS theory**  $\tau > 0, \tau_{\Omega} = 0.4ps, \tau_{\Theta} = 0.$

**Fig: 6(b).** Distribution of hoop stress component  $\sigma_{\theta\theta}(r, \theta, t)$  inside the hollow sphere for time-fractional derivative order  $\beta$  for  $\tau = \tau_{\Omega} - \tau_{\Theta} > 0, \tau_{\Theta} = 0.2ps, \tau_{\Omega} = 0.4ps.$

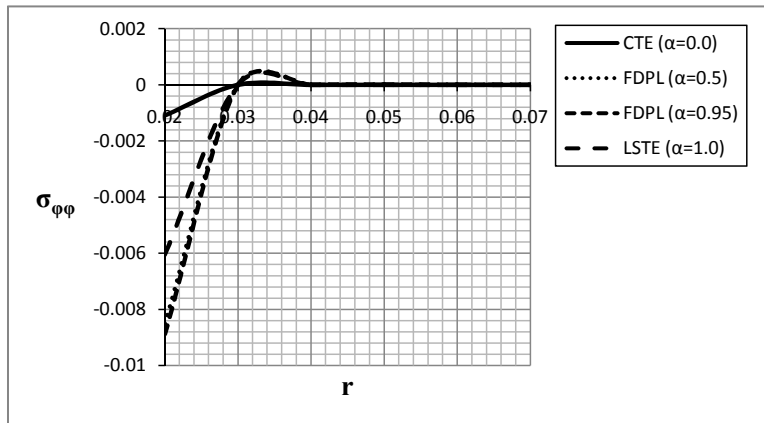
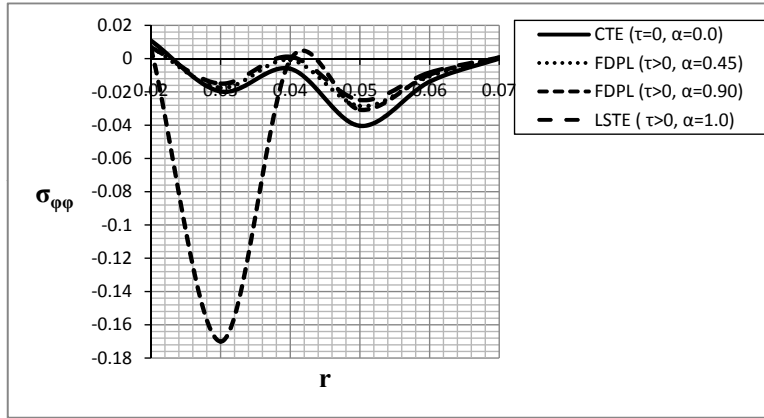


**Fig: 7(a).** Distribution of hoop stress component  $\sigma_{\phi\phi}(r, \theta, t)$  inside the hollow sphere for phase-lag variations

**CTE theory**  $\tau = 0, \tau_{\Omega} = \tau_{\Theta} = 0,$

**FDPL theory**  $\tau > 0, \tau_{\Omega} = 0.4ps, \tau_{\Theta} = 0.2ps, \beta = 0.45,$

**FDPL theory**  $\tau > 0, \tau_{\Omega} = 0.4ps, \tau_{\Theta} = 0.2ps, \beta = 0.90,$

**LS theory**  $\tau > 0, \tau_{\Omega} = 0.4ps, \tau_{\Theta} = 0.$

**Fig: 7(b).** Distribution of hoop stress component  $\sigma_{\phi\phi}(r, \theta, t)$  inside the hollow sphere for time-fractional derivative order  $\beta$  for  $\tau = \tau_{\Omega} - \tau_{\Theta} > 0, \tau_{\Theta} = 0.2ps, \tau_{\Omega} = 0.4ps.$

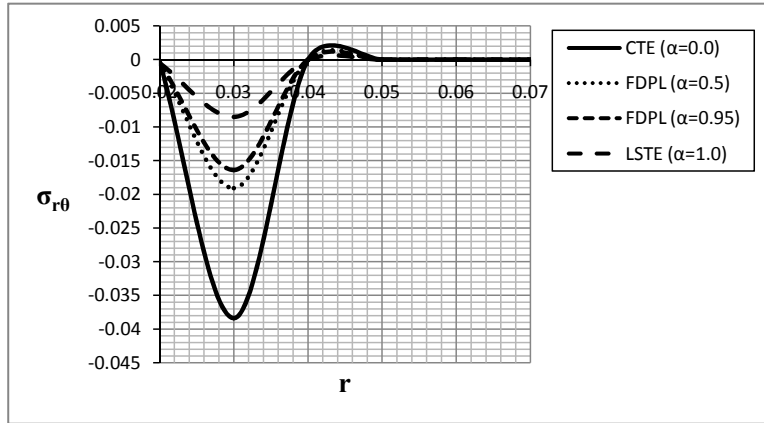
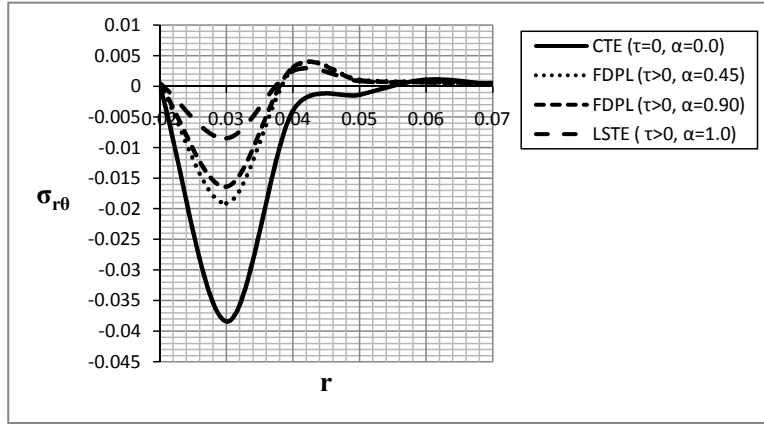


**Fig: 8(a).** Distribution of hoop stress component  $\sigma_{r\theta}(r, \theta, t)$  inside the hollow sphere for phase-lag variations

**CTE theory**  $\tau = 0, \tau_{\Omega} = \tau_{\Theta} = 0,$

**FDPL theory**  $\tau > 0, \tau_{\Omega} = 0.4ps, \tau_{\Theta} = 0.2ps, \beta = 0.45,$

**FDPL theory**  $\tau > 0, \tau_{\Omega} = 0.4ps, \tau_{\Theta} = 0.2ps, \beta = 0.90,$

**LS theory**  $\tau > 0, \tau_{\Omega} = 0.4ps, \tau_{\Theta} = 0.$

**Fig: 8(b).** Distribution of hoop stress component  $\sigma_{r\theta}(r, \theta, t)$  inside the hollow sphere for time-fractional derivative order  $\beta$  for  $\tau = \tau_{\Omega} - \tau_{\Theta} > 0, \tau_{\Theta} = 0.2ps, \tau_{\Omega} = 0.4ps.$

Figure 1(a) & 1(b), describes the variations of conductive temperature inside the hollow spherical region. It can be noticed from figure-1(a) that, whenever both phase-lags  $\tau_{\Omega}, \tau_{\Theta}$  are equal then FDPL model ex-

hibits results corresponding to the classical coupled theory of thermoelasticity (CTE). For a higher value of phase-lag corresponding to heat flux  $\tau_\Omega$  as compared to temperature gradient  $\tau_\Theta$ , it has been observed that the heat transfer takes place in a waveform with finite speed  $\sqrt{\frac{\Gamma(\beta+1)}{\eta\tau_\Omega^\beta}}$ . Wavefronts plotted in figure-1(b) shows that the conductive temperature corresponding to generalized theory is dominating over classical and fractional theory of thermoelasticity. Mathematically, it has been found that the conductive temperature is directly proportional to fractional order  $\beta$ .

Figure 2(a) & 2(b), illustrates the effect of variation of phase-lags  $\tau_\Omega, \tau_\Theta$  and fractional order  $\beta$  on thermodynamical temperature  $\vartheta(r, \theta, t)$  within the bounded spherical region. Results obtained are similar to those of classical coupled theory when the phase-lags are identically the same. If the phase-lag corresponding to heat flux vector precedes the phase-lag of temperature gradient ( $\tau_\Omega > \tau_\Theta$ ), then the wave fronts for fractional ( $\beta = 0.45, \beta = 0.90$ ) and generalized theories ( $\beta = 1.0$ ) are seems to be closer to each other. One may notice from the results shown by figure-2(b) that the thermodynamical temperature inside the solid is directly proportional to the fractional order  $\beta$  under consideration.

Figure 3(a) & 3(b), contains the wave fronts representing the non-dimensional radial displacement component  $u_r(r, \theta, t)$  for different values of phase-lags  $\tau_\Omega, \tau_\Theta$  and fractional order  $\beta$ . In both figures it has been shown that the radial displacement is merely increasing and becomes zero at the outer boundary. The results shown also explore the fact that the wave fronts corresponding to generalized theory ( $\beta = 1, \tau_\Omega > \tau_\Theta$ ) are fluctuating faster than the classical thermoelasticity theory ( $\beta = 0, \tau_\Omega = \tau_\Theta$ ). From figure-3(b), collectively it has been found that the radial displacement component variations are directly proportional to the fractional order  $\beta$ .

Figure 4(a) & 4(b), represents the angular displacement component  $u_\theta(r, \theta, t)$  within the hollow sphere. The displacement variation is increasing along radial distance and finally approaches to some non-zero value. Comparing the variations it could be seen that wave fronts corresponding to  $\tau_\Omega = \tau_\Theta$  are lagging to the wave fronts subjected to case  $\tau_\Omega > \tau_\Theta$ . The wave fronts obtained for fractional theory corresponding to  $\tau_\Omega > \tau_\Theta$  shows similar results. Moreover, the thermal investigations corresponding to various fractional orders by fixing phase-lags, it could be reasonably inferred that the displacement components are directly proportional to the fractional order  $\beta$ .

Figure 5(a) & 5(b), shows radial thermal stress variations for classical, fractional and generalized thermoelasticity theory considering various phase-lags and fractional orders are found to be compressive. It has been noticed in the results that stress variations are more inside the spherical region as compared to outer boundaries. Moreover, figures reveal that results obtained for fractional order  $\beta = 0.95$  are dominating as compared to classical and generalized theory. The traction free boundary condition is satisfied in both investigations.

Figure 6(a) & 6(b), exhibits hoop thermal stress  $\sigma_{\theta\theta}(r, \theta, t)$  variation for classical, fractional and generalized thermoelasticity theory considering various phase-lags and fractional orders. It has been found that the wave front expresses the tensile stress variations corresponding to  $\tau_\Omega = \tau_\Theta$  that shows negligible fluctuations however the significant fluctuations have been found for the wave fronts corresponding to  $\tau_\Omega > \tau_\Theta$ . Hoop stress component  $\sigma_{\theta\theta}$  is compressive for  $0 < r < 0.4$  and tensile for the rest of the region.

Figure 7(a) & 7(b), shows that the spherical boundaries are free of hoop stress  $\sigma_{\phi\phi}(r, \theta, t)$ . Hoop stresses are found to be compressive for  $0 < r < 0.3$ , however the wave fronts are quite close for classical  $\tau_{\Omega} = \tau_{\Theta}$  fractional and hyperbolic  $\tau_{\Omega} > \tau_{\Theta}$  theories except for one of the FDPL corresponding to  $\beta = 0.90$ . Observing figure 7(b), it can be observed that the hoop stress variations are found to be inversely proportional to fractional order applied to the model.

Figure 8(a) & 8(b), describes the shear thermal stress  $\sigma_{r\theta}(r, \theta, t)$  present inside the hollow sphere for classical, fractional and generalized thermoelasticity cases on varying the lags and fractional orders respectively. Graphically the results are similar and satisfying the traction free boundary conditions.

## 5. Conclusions

A well-posed fractionally ordered dual-phase-lag heat conduction model within the framework of two-temperature thermoelasticity theory has been derived in the presented manuscript. The generalized heat conduction equation (7) has been re-examined for several variations in phase-lags and fractional orders applied, depending upon the numerical values of phase-lags  $\tau_{\Omega}, \tau_{\Theta}$  and fractional order  $\beta$ , the classical coupled and generalized theory of thermoelasticity has been recovered.

Implementation of the delay time translations of heat flux vector ( $\vec{Q}$ ) denoted by  $\tau_{\Omega}$  and temperature gradient ( $\nabla T$ ) represented by  $\tau_{\Theta}$  where  $\tau = \tau_{\Omega} - \tau_{\Theta} > 0$ , converts the governing heat equation in the hyperbolic form, that leads to attain the definite speed of thermal wave propagation given by  $\sqrt{\frac{\Gamma(\beta + 1)}{\eta\tau_{\Omega}^{\beta}}}$ .

The formulation shown in the current article, revealed that several cases of early derived classical, coupled and generalized thermoelastic models have been found to be compatible with the presented model in the context of two-temperature theory.

Resulting time domain numerical values of several thermal parameters obtained in this fractional order DPL model derived in reference to the two-temperature theory are found to fulfill all the imposed physical restrictions prescribed in the given model for different values of fractional order and phase-lag variations.

Subjected to the hyperbolic ( $\tau_{\Omega} - \tau_{\Theta} > 0$ ) and parabolic ( $\tau_{\Omega} = \tau_{\Theta} = 0$ ) status of governing equation (13) remarkably distinguished outcomes have been detected for these two cases, moreover the couple of sets of results obtained for the phase-lag and fractional order variations are found to be closely similar to each other.

As per the resulting outcomes found in the given model, it is reasonably good to claim that fractional order of time derivative  $\beta$  and applied phase-lags  $\tau_{\Theta}, \tau_{\Omega}$  could be scientifically applied to classify distinct materials according to their capacity to conduct the heat.